# scientific reports



## OPEN

# Removal of reactive red 45 dye from aqueous solution using activated carbon developed from *Catha edulis* stem as a potential biosorbent

Tadele Mihret¹, Nigus Gabbiye¹, Bisratewongel Tegegne², Dessie Tibebe³ & Agegnehu Alemu²,⁴⊠

Textile dyes pose considerable environmental problems, as they often contain harmful chemicals that contaminate the soil and water sources. This study investigated the use of activated carbon made from Catha edulis stems, a waste product from leaf consumption, for the biosorption of reactive red 45 dye. The khat stems underwent a carbonization process followed by chemical activation using phosphoric acid. Various analytical techniques were used to examine the material's physical and chemical characteristics. Results showed that the activated carbon possessed diverse functional groups (FTIR), an amorphous internal structure with crystalline carbon regions (XRD), and a surface morphology featuring irregular shapes, pores, deep cavities, and holes (SEM). It also had a point of zero charge (pHpzc) of 4.82 and a high BET surface area of 496.316 m<sup>2</sup>/g. Batch adsorption experiments were conducted to assess dye removal efficiency and determine optimal removal conditions. The maximum removal efficiency of reactive red 45 dye was 94.5% under optimal conditions: pH 3.05, adsorbent dose 10.5 g/L, contact time 38.79 min, and an initial dye concentration of 50.4 mg/L. At these conditions, adsorption isotherm, kinetics, and thermodynamics were analyzed. The equilibrium data fit well with the Langmuir isotherm model and the pseudo-second-order kinetic model. These findings indicate that activated carbon developed from Catha edulis stem is a promising biosorbent for removing reactive red 45 dye from textile wastewater.

Environmental pollution is the main concern in the world at the present time. This is due to the rapid increase of industrialization, agriculture and population number, which consume a large amount of resources and generate wastes that pollute the environment. The wastes can be of different types, including organic and inorganic substances (heavy metal ions, pesticides, various types of dyes and other contaminants, which cause significant health hazards to living organisms and overall deterioration of the environment<sup>1–3</sup>. Water pollution poses serious concerns about human health and environmental risks in many developing countries, particularly those in Sub-Sahara, including Ethiopia<sup>4</sup>. Among those water pollutants dyes are the focus of many environmental concerns because of their non-biodegradable, complexity, and polluting nature, stability with highly resistant photolysis properties<sup>5</sup>.

Dyes are colored substance widely used in various industries such as textiles, paper, leather, plastics, food, cosmetics, pharmaceuticals, etc. to impart color to their products. They can be categorized into natural and synthetic types based on their origin<sup>6-8</sup>. Currently, several kinds of synthetic dyes are commonly used, including acid dyes, basic (cationic) dyes, direct dyes, reactive dyes, disperse dyes, vat dyes, and azo dyes. Despite their usefulness, dyes can pose serious risks to both the environment and human health. They can contaminate water bodies, lower oxygen levels, and endanger aquatic life<sup>9</sup>. Many dyes contain hazardous substances that are toxic, mutagenic, or carcinogenic, which may accumulate in the food chain<sup>10</sup>. Prolonged human exposure can cause respiratory problems, allergic reactions and cancer<sup>5</sup>.

<sup>1</sup>Faculty of Chemical and Food Engineering, Bahir Dar University, P.O Box 26, Bahir Dar, Ethiopia. <sup>2</sup>College of Science, Department of Chemistry, Bahir Dar University, P.O Box 79, Bahir Dar, Ethiopia. <sup>3</sup>Department of Chemistry, College of Natural and Computational Sciences, University of Gondar, P.O. Box 196, Gondar, Ethiopia. <sup>4</sup>Blue Nile Water Institute, Bahir Dar University, P.O Box 79, Bahir Dar, Ethiopia. <sup>△</sup>email: agegnehua@gmail.com

Textile industries consume a large quantity of dyes and release of effluents containing dyes in sufficient quantities<sup>11</sup>. Among them reactive dyes have a relatively low fixation rate (50–90%), with the remaining 10–50% being lost in the effluents<sup>12</sup>. Most reactive dyes are azo compounds, which are challenging to break down or remove and pose serious threats to aquatic ecosystems. Additionally, their breakdown products can be mutagenic and carcinogenic<sup>5,13</sup>.

Reactive red 45 dye (RR-45-D) is an anionic dye with chemical formula  $C_{27}H_{19}ClN_7Na_3O_{10}S_3$  and Molecular Weight 802.10 g/mol. It is a diazocompound which contain negatively charged sulfonic groups ( $SO_3^-$ ), highly soluble and visible in water bodies<sup>14</sup>. The structure of the molecule is shown in Fig. 1. RR-45-D has a strong interaction with many surfaces of synthetic and natural fabrics<sup>15</sup>. It is a widely used synthetic dye in the textile industries, due to shade versatility and good fastness besides its excellent binding property with fabric surfaces. Among all dyes, this dye generates the most pollution and became the major challenge in the world<sup>15</sup>.

Treatment of wastewater containing RR-45-D is very important to safe living organisms in the environment. There are different treatment methods and technologies commonly applied for dye removal in wastewater. This includes chemical oxidation, photocatalytic degradation<sup>16,17</sup>coagulation<sup>18</sup>filtration, ion exchange, adsorption, and biological treatment<sup>8,19</sup>. Among these wastewater treatment techniques, adsorption is found to be superior due to low initial cost, flexibility, and simplicity of design, ease of operation, and high removal efficiency<sup>10</sup>. Biosorbents are natural or modified materials used to remove pollutants, such as heavy metals, dyes, and other contaminants, from wastewater. They are typically derived from biomass materials like plants, agricultural byproducts, fungi, algae, or even microorganisms<sup>20,21</sup>. Biosorbents are effective in removing contaminants due to their large surface area, high porosity, and the presence of functional groups (such as hydroxyl, carboxyl, or amino groups) that interact with contaminants<sup>22,23</sup>. The efficiency of removal depends on nature of the contaminants, modification, and environmental conditions<sup>24</sup>. Biosorbents are low-cost, often use waste materials, and are reusable, though initial costs for modification or regeneration may add up. They are also considered highly sustainable, because they are made from renewable, biodegradable, and environmental friendly materials<sup>25,26</sup>.

Commercially available activated carbon is highly effective for the removal of dyes in wastewater. However, its use is limited due to its high cost<sup>8</sup>. Therefore, searching of low-cost biosorbents is very essential. In adsorption process several agricultural waste biosorbents have been reported including eggshell waste, rice hull ash, coffee grounds, coconut shell activated carbon, tobacco steam ash, fishery waste, vegetable residues, waste bamboo culms, and orange and banana peel<sup>7,27</sup>. *Catha edulis*, commonly referred to as khat, has attracted growing research interest as a potential cost effective adsorbent. This is primarily due to its abundant availability throughout the year in khat-producing regions, where large quantities of the stem are discarded as waste following the consumption of its fresh leaves. Furthermore, the presence of diverse functional groups on its surface enhances its suitability for adsorption applications<sup>1,28</sup>. In this study, activated carbon (AC) was produced from *Catha edulis* stems (CES) waste, which are often thrown away after use, thereby offering a sustainable approach to both waste management and material development.

The objective of this study was to investigate the adsorption of RR-45-D from aqueous solutions using AC developed from CES under various operational conditions, including pH, contact time, adsorbent dose, and initial dye concentrations. The study also explored adsorption isotherms, kinetics models, and thermodynamic properties related to the adsorption of RR-45-D onto the prepared AC biosorbent.

# Materials and methods Materials

The main raw material used in this study was CES waste used as a precursor for bio-adsorbent. Chemicals such as Phosphoric acid (85%, Thermo Scientific) was used for activation of CES powder, analytical grade Hydrochloric acid (37%, Fisher Scientific), and sodium hydroxide (98%, BDH chemicals) base were used for pH adjustment of the dye solution. Reactive red-45- dye powder ( $C_{27}H_{19}ClN_7Na_3O_{10}S_3$ ) obtained from Bahir Dar Textile Share Company was used as a model pollutant for the preparation of synthetic dye solution. Sodium chloride salt (98%, API manufacturer, India) was used for the determination of the point of zero charges and powdered anhydrous KBr (99.5%, Fisher scientific) was used to press the developed AC and obtain pellets for FTIR analysis to identify the functional groups of the biosorbent.

Fig. 1. The chemical structure of RR-45-D.

### Preparation of AC from CES

The biosorbent was prepared based on physical and chemical activation procedures with some modifications  $^{1,4,29,30}$ . The disposed CES was collected and washed with distilled water and dried in an oven (Italia, M40-VF) at 105 °C until it was completely dried. Then, it was crushed with a cutter mill (Germany, Fritsch, D-55743) for size reduction of the sample. The crushed CES was carbonized in a muffle furnace (Germany, Northern, L-030H<sub>2</sub>CN) at, 600 °C for one hour<sup>29</sup>. The chemical activation was carried out by taking 80 g weight of powdered carbonized sample and immersed in 12% phosphoric acid solution in the ratio of 1:5 (w/v) for 12 h. The soaked samples were filtered out by Whatman filter paper and washed with distilled water until the pH reached to neutral. The resulting biosorbent were completely dried at 105 °C in an oven for three hour. Finally, it was crushed and sieved in the range of 200–500 µm and stored in a plastic container for later use.

The point of zero charges (pH $_{pzc}$ )
The pH at which the Charge of the solid surface adsorbent is zero referred to as the point of zero charge (pH $_{pzc}$ ). The point of zero charge (pHpzc) of the biomass was determined by solid addition method<sup>1,15</sup>. 45 mL, 0.1 N of NaCl standard solution transferred in to a series of 100 ml of Erlenmeyer flasks. The initial pH of solution (pHi) were approximately adjusted from 2 to 12 by adding either 0.1 M HCl or 0.1 M NaOH. The total volume of the solution in each flask was made exactly to 50mLby adding the 0.1 N NaCl solution of the same strength. The initial pH of solution accurately noted and added 0.1 g of adsorbent to each flask and then securely capped immediately. The suspensions were shaken and allowed to equilibrate for 24 h. Finally; the final pH values of the supernatant liquid (pHf) were noted. The final pH values in y-axis were plotted against the initial pHi (x-axis). The point of intersection of the resulting curve with the x-axis gave the pHpzc.

### Analysis of surface area and porosity of AC developed from CES

Surface cleaning (degassing) was carried out using surface area and pore size analyzer (NOVA 4000e) by adding a samples of raw CES and both base and acid treated biosorbent separately in a glass cell and heating it under a vacuum for 30 min at 300 °c. After degassing, the glass cell, which contain sample, was transferred to Dewar flask, which contain liquid nitrogen and set up with computer to be analyzed. Then surface area, pore size and volume were analyzed by software, which is connected with instrument surface area and pore size analyzer (NOVA 4000e).

### Fourier transforms infrared (FT-IR), scanning electron microscopy (SEM) and X-ray diffraction (XRD) analysis of AC biosorbent

To determine the functional groups present in the bio-adsorbent, 2 mg of powdered sample was mixed with 300 mg of powdered anhydrous KBr, and then pressed to obtain the pellets. The spectra were recorded in the wavenumber range of 4000 and 400 cm<sup>-1</sup> using an FT-IR spectrometer (Perkin Elmer, FT/IR-6600). The surface morphology of the biosorbent was determined by using scanning electron microscope (SEM - JEOL, JSM 6360 LV). This was operated at 15 kv voltage and 1-3 nA beam current. The diffraction pattern of crystalline bioadsorbent was characterized by using a Bruker D2-phaser diffractometer (copper K $\alpha$  radiation,  $\lambda = 1.54056$  Å, with variable slits at 45 kV/40 mA). Scanning was done in the range of 10 to 75 (2θ) at a scanning rate of 2°  $min^{-1}$ .

### Batch adsorption experiment

1.0 gram of RR-45-D was mixed with 1 L of distilled water in order to prepare a 1000 mg/L synthetic stock dye solution. The varied concentrations of RR-45-D working solutions were prepared by dilution of the stock dye solution. Adsorption experiments were carried out in the batch mode according to 1,9,15 for optimizing the above different parameters with modification (Fig. 2). Solution pH (3-10), contact time (30-90 min), adsorbent dosage (0.5-1.5 g), initial dye concentration (50-100 mg/L), These batch adsorption experiments were conducted according to the run order of the design expert, as shown in Table 5 below, based on the CCD run order of the design expert. The experimental runs were conducted in a conical flask of 150 mL capacity. The experimental runs were conducted in a conical flask of 150 mL capacity. In all the experiments, the solution volume was 100 mL. The initial solution pH was adjusted using a pH meter by dropping 0.1 N HCl and 0.1 N NaOH before adding the required amount of adsorbent to the solution. The mixture solutions were agitated with a magnetic stirrer on a digital hot plate at 150 rpm until the necessary time was reached, and then the adsorbent was separated from the solution by filtration using Whatman filter paper No 42 (2.5 µm pore size). Finally, the absorbance of the supernatant solutions was assessed using a UV-Vis spectrophotometer (Lamda 35 Perkin Elmer) at the dye's maximum scanned absorbance of wave length of 542 nm. All experiments were performed according to experimental design layout.

### Experimental design by design expert

Statistical experimental design helps to optimize all affecting parameters easily compared to classical methods of studying adsorption processes. This approach helps to improve product yields, decreased process variability, closer confirmation of the output response to target requirements, shorter development times, and lower overall costs in the development of adsorption processes. The central composite design methodology was used to investigate the effects of process parameters, namely pH (A), adsorbent dose (B), contact time (C), and pollutant concentration (D), on the response and percentage of reactive red dye removal (Y). The result's significance was analyzed by analysis of variance (ANOVA). The 30 experiments were carried out, and the data was statistically analyzed by the Design-Expert software to find a suitable model for the percentage of reactive red dye removal yield as a function with the four factors shown in Table 1.

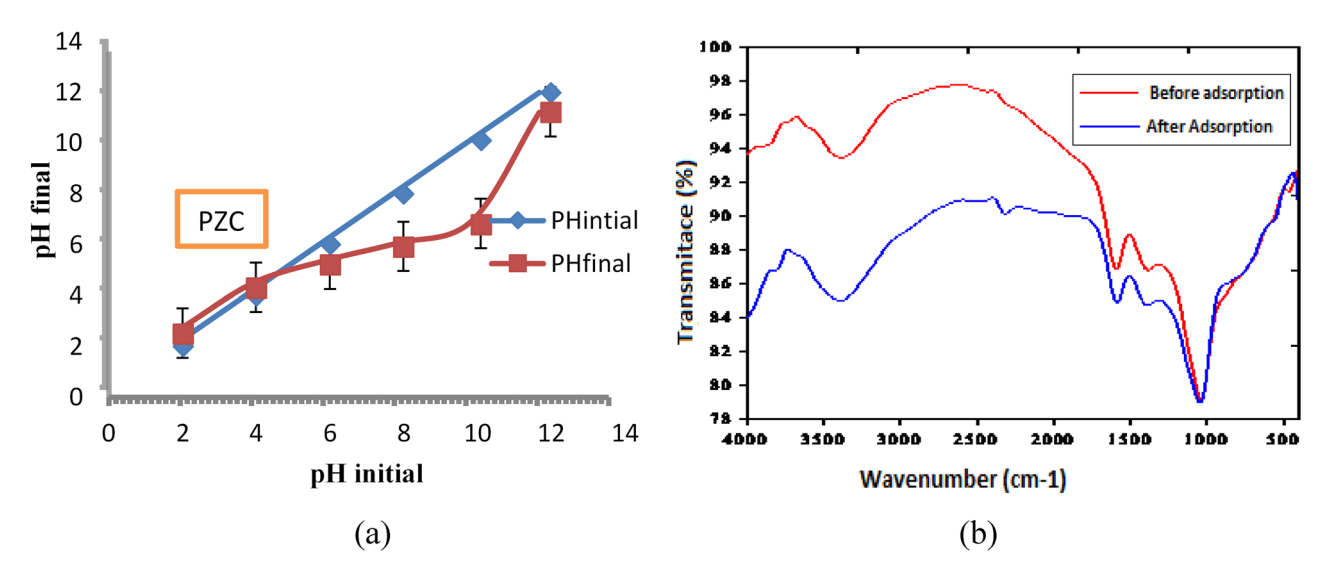


Fig. 2. Point of zero charge (PZC) (a); FT-IR spectra of AC of CES, before and after adsorption of RR-45-dye (b).

Process parameters	Code	Levels		
рН	A	3	6.5	10
Adsorbent dose (g/100mL)	В	0.5	1	1.5
Contact time (min)	С	30	60	90
Initial dye concentration (mg/L)	D	50	75	100

Table 1. Estimated factors and there levels employed for removal of RR-45-D.

The batch adsorption was evaluated under the percentage of dye removal, adsorption capacity, adsorption isotherm models, and thermodynamic properties.

Adsorption efficiency and capacity

The percentage of dye removal (% R) was determined using Eq. (1):

$$\% R = \frac{Co - Ce}{Co} * 100 \tag{1}$$

The adsorption capacity at equilibrium (q<sub>e</sub>) was determined by Eq. (2)

$$qe = \frac{(Co - Ce)v}{m} \tag{2}$$

Adsorption capacity at any time t (q,) was calculated via Eq. (3)

$$qt = \frac{(Co - Ct)v}{m}$$
 (3)

Where Co - initial dye concentration (mg/L);  $C_e$  - residual concentrations of the dye (mg/L) at equilibrium; V - volume of dye solution (L) and m - mass of the bio-adsorbents (g). Adsorption isotherms.

Biosorption isotherm models are applied on the adsorption process to know the type of adsorption, chemisorption or Physiosorption and can provide information about the maximum adsorption capacity of different adsorbents<sup>31</sup>. There are different isotherm models, the most commonly used are Langmuir and Freundlich models to describe the adsorption isotherm<sup>7</sup>.

The linear forms of Langmuir and Freundlich isotherm models are shown in Eqs. (4) and (5), respectively.

$$\frac{Ce}{Qe} = \frac{1}{bQm} + \frac{Ce}{Qm} \tag{4}$$

$$\log Qe = \log Kf + \frac{\log Ce}{n} \tag{5}$$

Where Qm is the maximum adsorption capacity of the adsorbent (mg  $g^{-1}$ ), and b is the Langmuir constant (L mg $^{-1}$ ) & Kf is Freundlich constant (L kg $^{-1}$ ). The isotherm parameters b and Qm were determined from the intercept and the slope of Ce/qe versus Ce graph. The constants 1/n and Kf are obtained from the slope and intercept of the Freundlich model plot of log Qe vs. log Ce graph.

The Langmuir isotherm can be expressed in terms of a dimensionless constant termed as separation factor  $(R_L)$  given by the equation below (Eq. 6) that can be used to determine the feasibility of adsorption in a given concentration range over adsorbent<sup>1,7,15</sup>. The RL value indicates the types of adsorption to be either unfavorable if  $R_1 > 1$ , favorable if  $0 < R_1 < 1$ , linear if  $R_1 = 1$ , and irreversible if  $R_1 = 0$ .

$$RL = \frac{1}{1 + bCo} \tag{6}$$

The Temkin isotherm model suggests that the surface coverage, which occurs due to the interaction between the adsorbent and adsorbate, leads to a linear reduction in the heat of adsorption. The linear Temkin isotherm model is represented by the Eq.  $(6)^{32}$ .

$$Q_e = \frac{RT}{b_T} \ln k_T + \frac{RT}{b_T} \ln Ce \tag{7}$$

R is the universal gas constant (8.314 J/mol. K), T is the absolute temperature (K),  $k_T$  is the equilibrium binding constant (L/g),  $b_T$  is the Temkin constants (J/mol).  $b_T$  is calculated from the slope of the graph of Qe Vs ln(Ce), and  $k_T$  is calculated from the intercept.

### Kinetics study

Adsorption rate is very important to design the adsorption system. To determine the rate of uptake of adsorbate on the adsorbent surface, different kinetic models have been used to analyze the experimental data. Two most common kinetic models were used including pseudo-first-order and pseudo-second-order. The linear equations of pseudo-first-order and pseudo-second-order models are given in Eq. (8)<sup>33</sup> and (9)<sup>34</sup>respectively.

$$log (qe - qt) = log qe - k1$$
 (8)

$$\frac{t}{qt} = \frac{1}{K_2 q e^2} + \frac{t}{q e} \tag{9}$$

Where k1 is the rate constant of pseudo-first-order ( $min^{-1}$ ) and t is the contact time (min). Whereas K2 is the kinetic rate constant (g/mg h) of pseudo-second-order. K1 is obtained from the plot of log (qe-qt) Vs t and K2 is obtained from plot t/q, versus t.

### Thermodynamic study

Thermodynamic study shows the favorability and feasibility of the adsorption process by determine thermodynamic parameters. The thermodynamic parameters such as enthalpy ( $\Delta H$ ), entropy ( $\Delta S$ ), and Gibbs free energy ( $\Delta G$ ) was evaluated to understand the effect of temperature on adsorption and also the spontaneity of the adsorption process. Those parameters were calculated by applying the following Eqs. (10-13)<sup>35</sup>.

$$\Delta G = \Delta H - T\Delta S \tag{10}$$

$$\Delta G = -RTLnK \tag{11}$$

$$Kc = \frac{qe}{ce} \tag{12}$$

$$LnKc = \frac{\Delta S}{R} - \frac{\Delta H}{RT}$$
 (13)

Where R is Gas constant with a value of  $8.314 \text{ J mol}^{-1}\text{K}$ , T is absolute temperature (K). Kc is equilibrium constant;  $\Delta H$ ,  $\Delta S$  and  $\Delta G$  are Changes in enthalpy, entropy, and Gibbs free energy respectively. The values of  $\Delta H^{\circ}$  and  $\Delta S^{\circ}$  are determined from the slope and intercept of the linear plot of (Ln KC) versus (1/T).

### Statistical analysis

The adsorption of RR-45-D onto activated CES was examined through multiple statistical and modeling approaches to assess adsorption efficiency, kinetics, isotherm behavior, and thermodynamic properties. All experiments were conducted in triplicate, and results are presented as mean  $\pm$  standard deviation. Statistical significance was determined at a confidence level of 95% (p<0.05), using SPSS software version 27.

### Results and discussion Characterization of AC developed from CES

Brunauer-Emmett-Teller (BET) analysis

The carbonized product at 600 °C for one hour was activated by using  $\rm H_3PO_4$  and NaOH in order to increase specific surface area, remove tar formation, and fixed during carbonizations as to increase the removal efficiency of the bio-adsorbent (Table 2).

The BET surface areas analysis of carbonized raw CES, base-activated CES, and acid- activated CES were found to be  $281.619 \text{ m}^2/\text{g}$ ,  $413.401 \text{ m}^2/\text{g}$ , and  $496.316 \text{ m}^2/\text{g}$ , respectively. The increment in this surface area is due to the effect of the activating agent  $^{36}$ . Based on these responses acid treated activated carbon was selected for further analysis & removal of RR-45-D in aqueous solution.

### Point of zero charge (PZC) of the biosorbent

PHpzc is an important property of an adsorbent that can determine the surface charge behavior of the adsorbent. The pH of point zero charge of the AC biosorbent was found 4.82 (Fig. 2 (a)). If pH=pHpzc, the surface of the adsorbent becomes neutral charge. If pH < pHpzc, the biosorbent surface is a net positive charge, while at pH > pHpzc, the surface charge on the adsorbent is a net negative charge<sup>37</sup>. The surface of biosorbent bears a net positive charge below pH < 4.82. The surface of the biosorbent bears a net negative charge above pH > 4.82. The PZC plays an important role for adsorption of reactive red 45 dyes on the biosorbent.

### FT-IR analysis

The FTIR analysis of the developed AC biosorbent before and after adsorption is shown in Fig. 2(b). The peak occurred between 3350 and 3400 cm<sup>-1</sup> indicates the presence of hydroxyl functional groups which could be associated from the building block of the material, absorbed moisture, and phenol functional groups  $^{1,4}$ . Another peak was observed between 1500 and 1700 cm<sup>-1</sup>, this may be due to the presence of C=C in aromatic ring and carbonyl functional group. The peak at 1606 and 1032 cm<sup>-1</sup> indicated for C=C stretch in aromatic ring and C=O starching, respectively. The sharp peaks produced at 1068 cm<sup>-1</sup> before and after adsorption indicate the presence of phosphate functional group. When we compare FTIR spectra obtained before and after adsorption, the peak intensity and position around 1068 cm<sup>-1</sup> is nearly the same indicating little or no adsorption of the dye but there are some difference in the intensity of wave numbers before and after adsorption. The change in the C=C stretching vibration from 1601.41 to 1602.73 cm<sup>-1</sup> indicates possible  $\pi$ - $\pi$  interactions between RR-45-D and the aromatic rings in the activated CES<sup>38</sup>. Additionally, the shift in the peak from 1265 to 1300 cm<sup>-1</sup> after adsorption implies that hydrogen bonding occurs between the C-O and -OH groups in the activated carbon and RR-45-D<sup>39</sup>.

### SEM analysis

SEM is frequently used to examine adsorbent materials' surface properties and morphological features. The SEM images before and after activation of the carbonized CES is shown in Fig. 3(a) and (b), respectively. The photograph shows that the carbon before activation is packed, poreless, and contains some irregularities but no cavities or cracks. However, the surface of the AC shows the existence of several irregularities, porosities, deep cavities, and holes. Due to the removal of volatile matter by carbonization and the activating agent<sup>40,41</sup>. This property of the AC can enhance its adsorption capacity of RR-45-D.

### XRD analysis

Xray diffraction (XRD) was used to determine the crystalline nature and composition of the prepared adsorbent. This bio-adsorbent was scanned within a diffraction angle of  $2\theta$  in the range of  $2^{\circ}$  to  $80^{\circ}$ . The XRD peaks of the biosorbent are shown in Fig. 4. The highest sharp and intense peak of the AC biosorbent was recorded at about  $2\theta$  angle of  $26.5^{\circ}$ . This shows a crystalline carbonaceous structure of the AC of CES, which contains phosphorus Oxo nitride (NOP)<sup>42</sup>. The small peaks recorded at  $21^{\circ}$  and  $51^{\circ}$  indicates the presence of SiC crystal structures<sup>43</sup>. The prepared biosorbent also indicates the presence of amorphous structures in the bulk body of the material. This amorphous nature of the biosorbent contributes to have higher surface area which results for better adsorption.

### Effects of adsorption parameters

In this study, the effects of pH, adsorbent dosage, contact time, and RR-45-D concentration by using the prepared AC as biosorbent on the removal efficiency of RR-45-D were investigated and optimized in the Bach adsorption system. Experimental runs and their corresponding removal efficiencies were performed (Table 9). The removal efficiencies obtained were in the range of 94.5 to 19.27%. The maximum removal efficiency was obtained on adsorbent dosage of 1.5 g, contact time 90 min, pH 3 and initial dye concentration 50 mg/L. On the other hand,

Name of sample	Sample weight	Degas temp	Degas time	SBET m <sup>2</sup> /g
Raw carbonized CES	0.09 g	300 °C	30 min	281.619
Activation with NaOH	0.09 g	300 °C	30 min	431.401
Activation with H <sub>3</sub> PO <sub>4</sub>	0.09 g	300 °C	30 min	496.316

**Table 2.**  $S_{BET}$  parameters of base and acid activated samples.

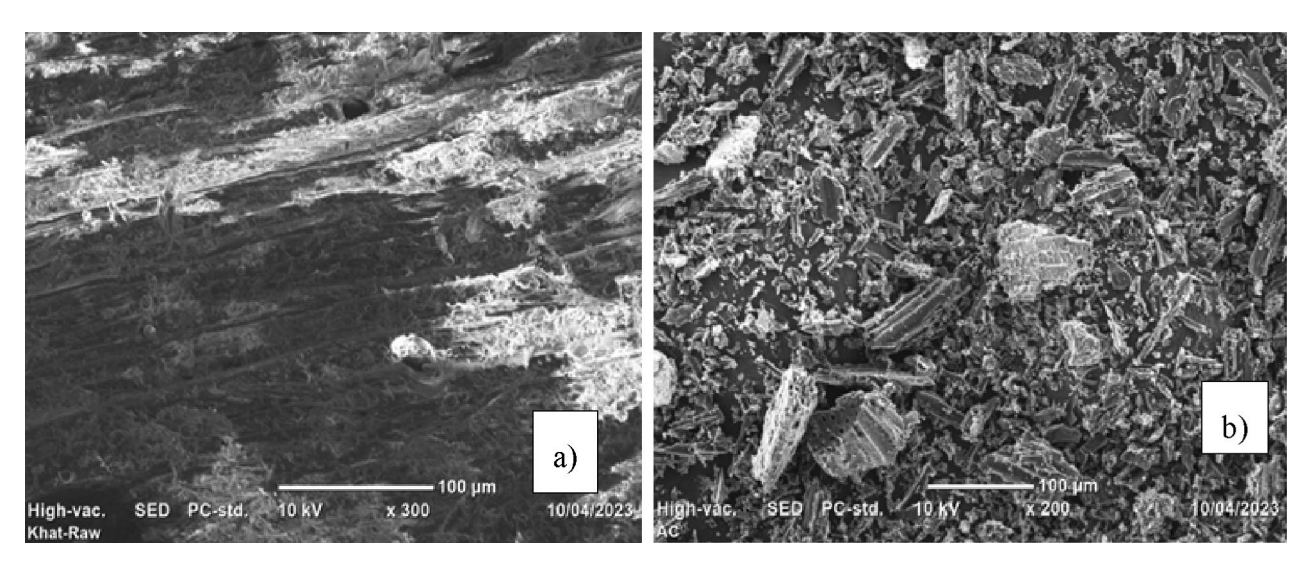


Fig. 3. SEM observation of a) raw, b) acid AC of CES.

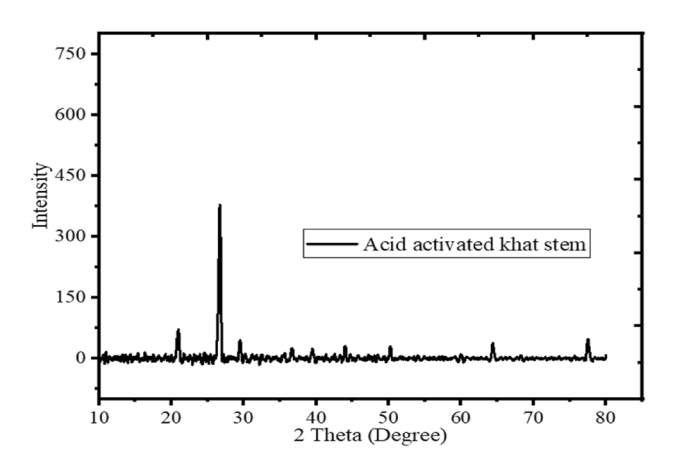


Fig. 4. XRD diffraction spectra of AC of CES.

minimum removal efficiency was obtained on the adsorbent dosage of 0.5 g, contact time 30 min, pH 10, and initial dye concentration  $100 \text{ mg/L}^{15}$ .

### Model validation and statistical analysis of the experimental results

In this study, the adsorption experiments for RR-45-D were planned using Response Surface Methodology (RSM) with a Central Composite Design (CCD), considering four variables: pH (A), adsorbent dose (B), contact time (C), and pollutant concentration (D). The experimental design included 30 runs and was developed using Design-Expert software version 13.0 (Table 3). The model summery statistics focus on, the model maximizing the Adjusted  $\mathbb{R}^2$  and predicted  $\mathbb{R}^2$ . So that according to central composite design (CCD) fit summary analysis quadratic model is suggested due to large value of predicted  $\mathbb{R}^2$  from the rest of other models (Table 4).

The Predicted  $R^2$  value of 0.9681 shows reasonable agreement with the Adjusted  $R^2$  value of 0.9886, as the difference is less than 0.2. This indicates that experimental result agrees well with the predicted values. Additionally, the distribution of actual and predicted values closely follows a straight line, indicating a good fit of the model with the experimental data, as illustrated in Fig. 5. The statistical significance of the model and process variables was analyzed using ANOVA, as shown in Table 5.

The P values are used as a tool to check the significance of the model and the factors using the data obtained from the experiment and the mutual interactions between the test variables. There is only a 0.001% chance that an F value this large could occur due to noise. The model P value is very low (<0.05). This indicates that the model is significant. The ANOVA result shows that the above model is appropriate to predict the removal efficiency of AC of CES biosorbent for RR-45-D. According to the ANOVA results, pH, adsorbent dose, contact time, and initial pollutant concentration were dominant factors affecting the biosorption of RR-45-D by current prepared bio-adsorbents because the p value was less than 0.05.

	Factor	1=pH; Factor 2=adsorb tration	; Factor 4 = pollutant	Actual value	Predicted value	
Run	A: pH	B: adsorbrent dose (g)	C: contact time (min)	D: initial dye conc. (mg/L)	(% removal)	(% removal)
1	3	0.5	90	50	86.78	86.70
2	6.5	0.5	60	75	46.92	47.37
3	10	1.5	90	100	36.14	37.07
4	6.5	1	30	75	51.62	53.07
5	10	1	60	75	43.61	46.82
6	10	1.5	90	50	59.33	59.08
7	3	1.5	90	100	60.06	58.11
8	10	1.5	30	50	52.14	51.73
9	3	0.5	90	100	40.71	42.85
10	3	1	60	75	79.69	77.37
11	10	0.5	90	50	47.05	46.63
12	3	1.5	30	50	89.27	88.67
13	6.5	1	60	75	59.21	59.23
14	10	0.5	30	100	19.27	19.46
15	10	1.5	30	100	34.83	32.95
16	6.5	1	60	75	62.26	59.23
17	6.5	1.5	60	75	58.34	58.79
18	6.5	1	60	50	78.03	77.44
19	10	0.5	30	50	44.17	44.16
20	6.5	1	60	100	44.63	46.12
21	3	0.5	30	100	45.29	43.58
22	6.5	1	90	75	56.94	56.38
23	6.5	1	60	75	59.21	59.23
24	3	0.5	30	50	83.39	84.20
25	6.5	1	60	75	59.21	59.23
26	10	0.5	90	100	20.06	18.70
27	3	1.5	30	100	51.82	53.97
28	6.5	1	60	75	60.17	59.23
29	3	1.5	90	50	94.5	96.05
30	6.5	1	60	75	57.99	59.23

Table 3. Adsorption experiment runs and corresponding response removal efficiency.

Source	Sequential <i>p</i> -value	Lack of Fit p-value	Adjusted R <sup>2</sup>	Predicted R <sup>2</sup>	
Linear	< 0.0001	0.0030	0.9207	0.8931	
2FI	0.0297	0.0068	0.9467	0.9021	
Quadratic	< 0.0001	0.1828	0.9886	0.9681	Suggested

Table 4. Model fit summary response 1 % removal efficiency RR-45-D.

### Effect of pH

The effectiveness of biosorbents can be significantly impacted by the pH of the solution (Table 4). This is due to the fact that the pH can impact how charged the molecules of the adsorbent and adsorbate are, which can affect the biosorbent's capacity and selectivity for adsorption. The impact of pH on the RR-45-D removal was investigated at pH 3, 6.5 and 10. The highest percentage of reactive red dye was removed at lower pH values, whereas the lowest percentages were removed at higher pH values. The produced material has a pH $_{\rm PZC}$  value of 4.82, and the highest RR-45-D percentage removal occurred at a pH level below the pH $_{\rm PZC}$  value. Because the biosorbent surface becomes cationic due to protonation of H $^+$  of the biosorbent at low pH conditions, which increases its reaction with the anionic sulphonate of the dye. But the minimum RR-45-D removal happens at pH above the pH $_{\rm PZC}$  value or at basic media because the biosorbent becomes negative charge on the surface and OH $^-$  can compete with the RR-45-D ions for the active surface sites $^{37}$ . The results of the present study are consistent with other studies. So due to the existence of electrostatic attraction and electrostatic repulsion forces between biosorbent and pollutant material, removal efficiency was highly varied $^{1,19}$ .

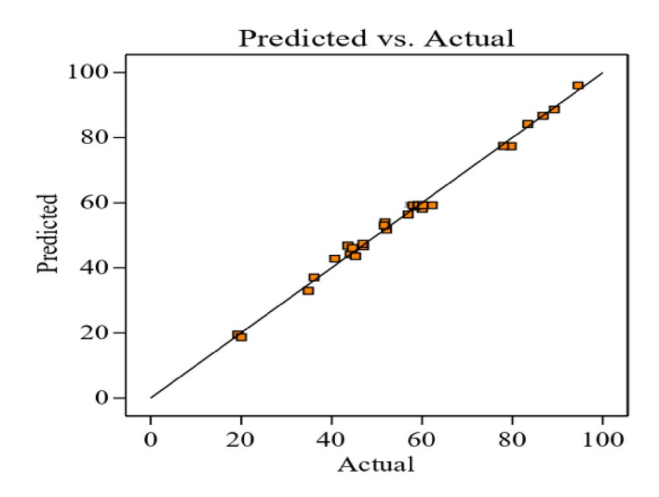


Fig. 5. Plot of the predicted data versus the experimental data of RR-45-D adsorption.

Source	Sum of Squares	df	Mean Square	F-value	p-value	Significance
Model	9868.41	14	704.89	180.02	< 0.0001	S
A-pH	4198.64	1	4198.64	1072.31	< 0.0001	S
B-adsorbent dose	586.99	1	586.99	149.91	< 0.0001	S
C-contact time	49.24	1	49.24	12.57	0.0029	S
D-pollutant con.	4413.30	1	4413.30	1127.13	< 0.0001	S
AB	9.63	1	9.63	2.46	0.1378	NS
AC	0.0008	1	0.0008	0.0002	0.9891	NS
AD	253.37	1	253.37	64.71	< 0.0001	S
ВС	23.74	1	23.74	6.06	0.0264	S
BD	35.02	1	35.02	8.94	0.0091	S
CD	10.45	1	10.45	2.67	0.1232	NS
A <sup>2</sup>	21.33	1	21.33	5.45	0.0339	S
B <sup>2</sup>	98.02	1	98.02	25.03	0.0002	S
C <sup>2</sup>	52.48	1	52.48	13.40	0.0023	S
$D^2$	16.84	1	16.84	4.30	0.0557	NS
Residual	58.73	15	3.92			
Lack of Fit	48.32	10	4.83	2.32	0.1828	NS
Pure Error	10.42	5	2.08			
Cor Total	9927.15	29				

Table 5. Analysis of variance for the removal efficiency. S denotes significant & NS to non-significant.

### Effect of adsorbent dose

The biosorbent dose is a crucial variable, since it affects the biosorbent's capacity for a specific initial concentration of the adsorbate. Biosorbent dosage for this investigation ranged from  $0.5\,\mathrm{g}/100\,\mathrm{mL}$  to  $1.5\,\mathrm{g}/100\,\mathrm{mL}$ . In this study the maximum removal efficiency of RR-45-D was achieved at an adsorbent dosage level of  $1.0\,\mathrm{g}/100\,\mathrm{mL}$ . After that, the removal efficiency becomes almost remained constant (Table 4). The increase in the removal efficiency with an increase in the dosage is due to the availability of greater surface area and more adsorption sites<sup>40</sup>.

### Effect of initial RR-45-D concentration

A given mass of adsorbent can only absorb a fixed amount of adsorbate. The adsorbate solution's initial concentration is crucial for studying adsorption experimentally. For the current experiment, initial RR-45-D concentrations ranging from 50 mg/L to 100 mg/L were employed. The greatest removal efficiency for RR-45-D was observed at 50 mg/L (Table 4). This can be explained by the fact that when present in low concentrations, the pollutant ions interact with the binding sites, resulting in maximum adsorption. This is because the ratio of the accessible surface to the initial concentration of pollutant ions is higher at low concentrations, when removal is more effective. More RR-45-D ions were not adsorbed when the concentration was higher. Generally, as the RR-45-D concentration increases, the tendency of the dye ions also increases to associate themselves in an aqueous solution at higher concentrations increases, and as a result, the removal efficiency decreases. This result is consistence with reported previous study<sup>15</sup>.

### Effect of contact time

The contact time also have an influence on the percentage of RR-45-D removal as shown in Table 4. As the contact time varies from 30 to 90 min by keeping constant other parameters. It was observed that removal of RR-45-D by the prepared bisorbent increased initially. It appears that after a period of time the removal efficiency was constant<sup>44</sup>. This is unsurprising as a large number of vacant surface sites are available high for adsorption during the initial stage and after a time the remaining vacant surface sites are difficult to occupy due to blocked the active sites and occupied with no chance for other adsorbates to be removed.

### Interaction effect of adsorption process variables

2D and 3D contour response surface plots for the measured responses were constructed to better find out about the impacts of independent parameters and their interactions with the dependent ones. The 3D response surface plots and the 2D contour plots below showed the relative effects of each of the two variables on the removal efficiency of RR-45-D on the prepared bio-adsorbent. Individually, the removal efficiency of the prepared bio-adsorbent for RR-45-D removal increased with the increase of the adsorbent dose and contact time, while it decreased with the increase of the pH and initial RR-45-D concentration. An interaction occurs when the response is different depending on the settings of two factors. Plots make it easy to interpret two-factor interactions on removal efficiency. There are three interaction factors analyzed by the model (Table 5). Those are: AD (pH and initial dye concentration), BC (adsorbent dose and contact time), and BD (adsorbent dose and initial dye concentration). This interaction has a significant effect on the response because their p-value is less than 0.05, but other variable interaction effects have no significant effect on the response.

### Interaction effect of pH and initial dye concentration

The interaction effect of pH and RR-45-D concentration is shown in Table 4 at the center point of the adsorbent dose and contact time. The percent removal of RR-45-D increases with decreasing pH at lower concentrations. At lower pH, the surface becomes positive charge, which is good for dye removal, and at the same time, at lower dye concentrations, the adsorbent active site is more active. The interaction of pH and initial dye concentration has a synergetic effect on dye removal Fig. 6a,b.

### Interaction effect of adsorbent dose and initial dye concentration

Figure 6 (c & d) depicts the 2D and 3D surface plot on dye removal efficiency as function of initial dye concentration (D) and adsorbent dose (B) at constant pH and contact time. It was observed that there was sharp improvement on dye removal efficiency when the adsorbent dose increases from 40 to 78%. This is due to the fact that when the adsorbent dose is increased, the active sites of biosorbent increased, which could adsorb more dye ions.

### **Optimization process**

In this study optimum operating conditions were searched to maximize the removal efficiency of RR-45-D (Fig. 6(e)). In the optimization process, the desired goal was chosen for each factor and response from the menu. The possible goals are maximize, minimize, target, within range, none (for responses only), and set to an exact value (factors only). A numerical response method was applied for optimization of any combination of five goals, namely pH, initial RR-45-D concentration, adsorbent dosage, contact time and removal efficiency. In optimization analysis, the targeted criteria set as maximum values for response while the values of the variables were set within the ranges. The software searched for combination of factors that simultaneously satisfied the requirement placed on the ultimate goal of the response and each of the factors. The goals were composed into an overall desirability function. In order to verify optimization result an experiment was performed under predicted condition by the developed model<sup>45</sup>. The model predicted 94.99% removal of RR-45-D at pH 3, adsorbent dose 1.05 g/L, RR-45-D concentration 50.46 mg/Land contact time 38.79 min from 100 mL solutions and the experimental value obtained at these conditions is 94.5%. It was observed that experimental value obtained were good agreement with the values predicted from the models.

### Adsorption isotherm study

Adsorption isotherms of RR-45-D on the developed AC biosorbent surface under the optimal conditions were investigated. The applicability of isotherm models for the removal of RR-45-D was analyzed by using the equilibrium data obtained from batch adsorption experiments by using Eq. 8 for Langmuir and Eq. 9 for Freundlich models. Isotherm parameters for each respective model are shown in Table 6. The Langmuir model showed the highest correlation coefficient ( $R^2$ ) 0.9986 (Fig. 7 (a)). This indicates that Langmuir isotherm model fits well the experimental data and verifies the monolayer coverage of RR-45-D onto the prepared AC biosorbent ( $Q_m = 7.94 \, \text{mg/g}$ ) with a homogeneous distribution on the adsorbent surface. The High surface area of the Ac obtained may come from a large number of micropores. This can agglomerate or pack poorly, causing mass

Adsorbent	Langmuir model			Freundlich model Temkin Model						
AC	Qm	b	R2	$R_L$	kf	n	R2	b <sub>T</sub>	K <sub>T</sub>	R2
AC	7.94	0.454	0.9986	0.042	3.636	4.43	0.996	0.996	1.3	0.9954

**Table 6**. Langmuir, Freundlich, and Temkin isotherm parameters of adsorption of RR-45-D on the surface of AC of CES.

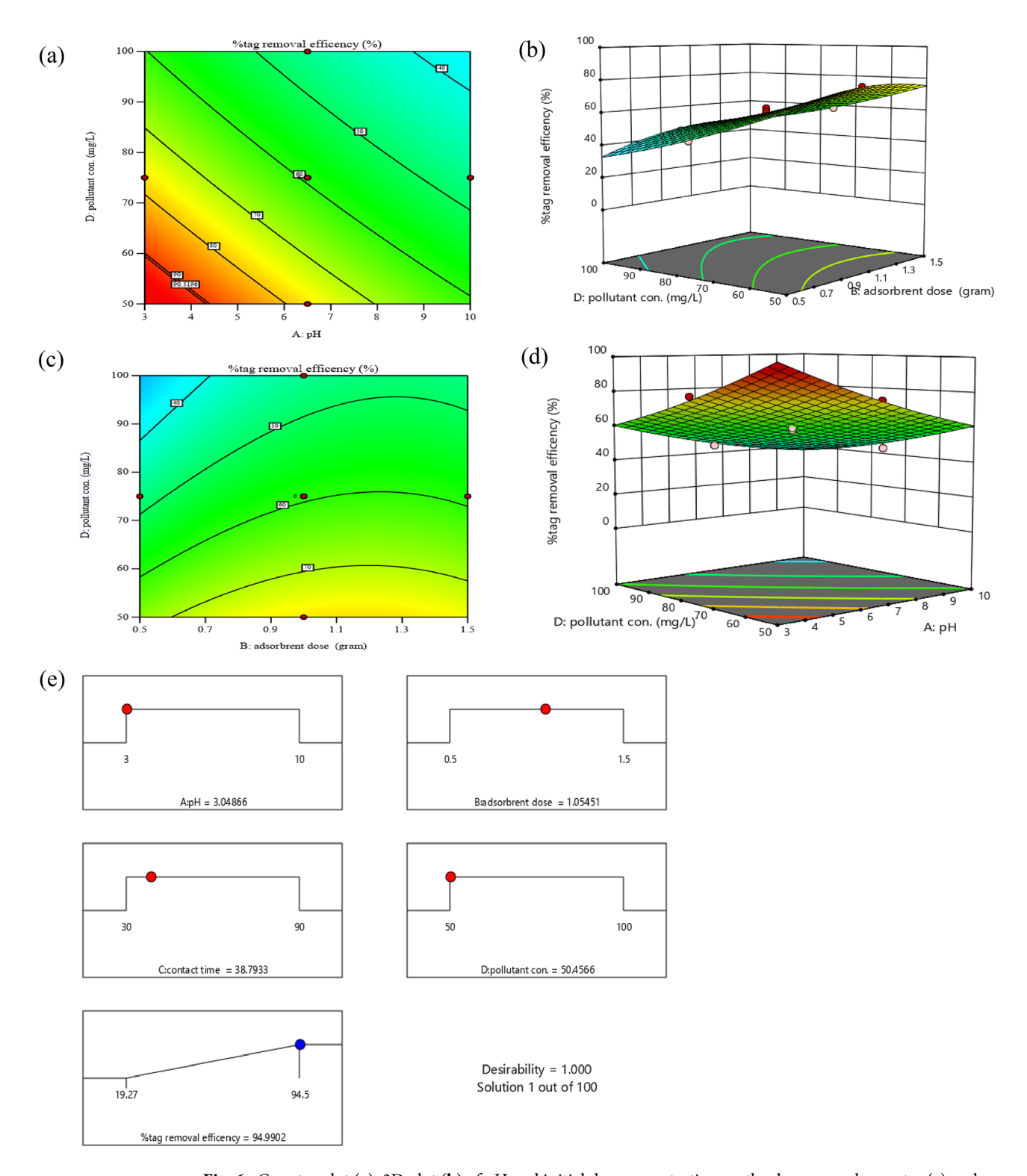


**Fig. 6.** Counter plot (**a**), 3D plot (**b**) of pH and initial dye concentration on the dye removal; counter (**c**) and 3D plot (**d**) interaction effect of adsorbent dose and dye concentration; Ramp desirability (**e**).

transfer limitations and low practical uptake. The separation factor ( $R_L$ ), was calculated using Eq. 10, to get information about the favorability of adsorption of RR-45-D onto the AC biosorbent. The  $R_L$  value was found 0.0423. This indicates that the adsorption of RR-45-D on the surface of the developed AC biosorbent is favorable. The Freundlich isotherm model showed a correlation coefficient ( $R^2$ ) of 0.996 (Fig. 7 (b)). Although this  $R^2$  value is slightly lower than Langmuir model, the data fit well with it too. The adsorptive intensity (n) was found 4.43, which indicates that the surface is good for adsorption  $R^4$ . The high  $R^2$  values of the Freundlich model indicates that the adsorption process probably involves multiple mechanisms, including multilayer adsorption (physical

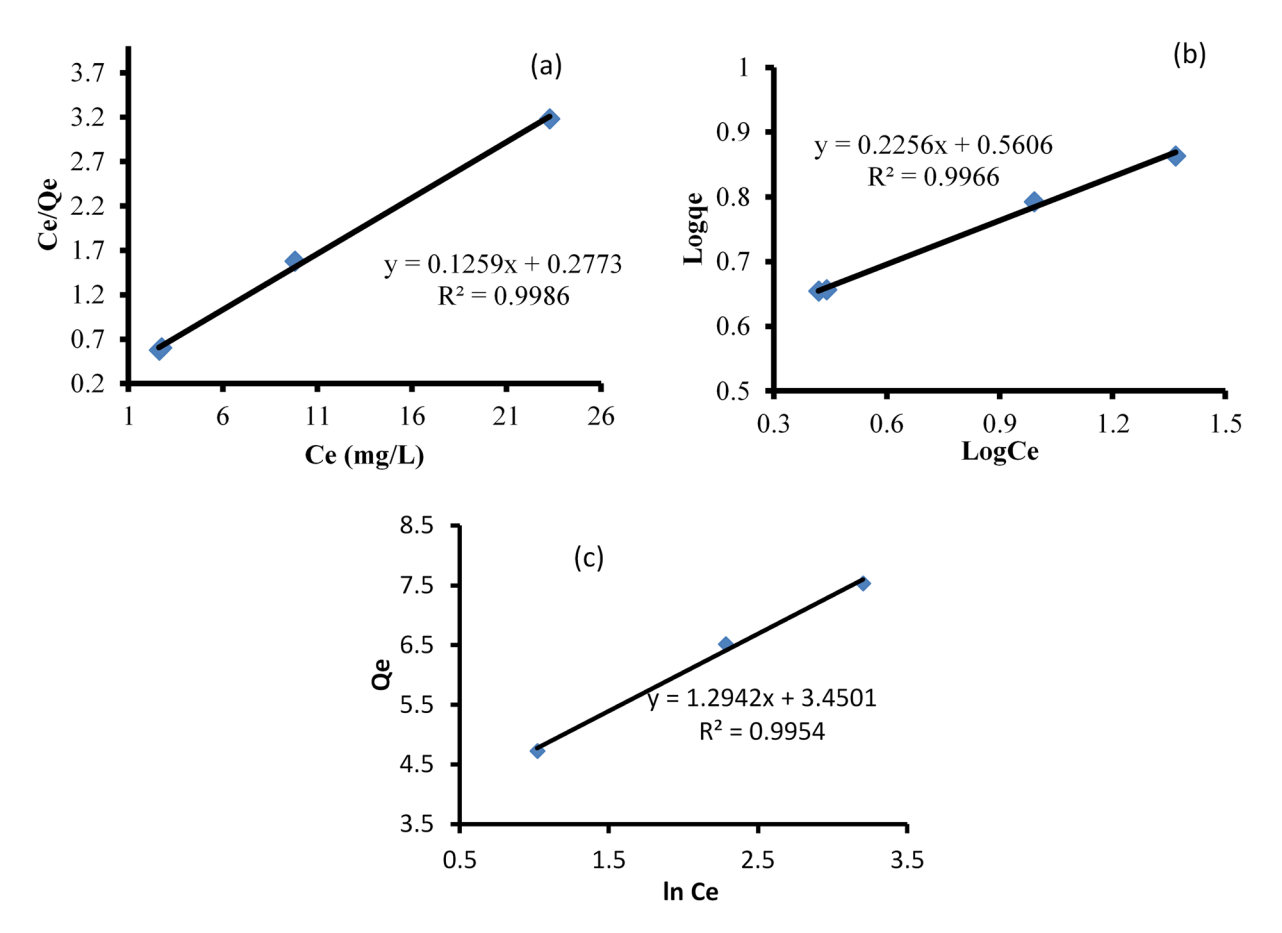


Fig. 7. Langmuir (a), Freundlich (b), and Temkin (c) isotherms for adsorption of RR-45-D onto AC of CES.

Time(min)	Ce(mg/L)	Qe(mg/L)	Qt(mg/L	Log(Qe-Qt)	t/Qt
30	7.654	4.538	4.071	-0.331	7.369
60	2.882	4.538	4.526	-1.905	13.258
90	2.817	4.538	4.532	-2.206	19.86

Table 7. Adsorption kinetics values.

C <sub>o</sub> (mg/L)	Q <sub>exp (mg/g)</sub>	Pseud	o first or	der	Pseudo second order			
50	4.54	Q <sub>cal</sub>	K1	R <sup>2</sup>	Q <sub>cal</sub>	K2	R <sup>2</sup>	
50	4.54	4.54	0.0313	0.8668	4.8	0.043	0.998	

**Table 8**. Pseudo first order and pseudo second order kinetics for adsorption of RR-45-D on the AC of CES.

interactions)<sup>34</sup>. The Temkin isotherm model showed correlation coefficient of (R<sup>2</sup>) of 0.9954 (Fig. 7(c)). The Temkin isotherm constants  $K_T$  and  $b_T$  are determined to be 14.37 L/g and 1.29 J/mol, respectively. The positive  $b_T$  value implies that the adsorption process of RR-45-D onto the developed AC biosorbent is exothermic<sup>47</sup>.

### Kinetics adsorption study

The kinetics of RR-45-D adsorption onto AC biosorbent using pseudo first order and pseudo second order kinetic models are illustrated in Table 7 and Fig. 8a,b.The correlation coefficients ( $R^2$ ) of pseudo first order and pseudo second order kinetic models are 0.8668 and 0.998, respectively. This indicates that pseudo-second-order model fitted well with the experimental data. Moreover, the value of the experimental adsorption capacity  $Q_{\rm exp}$  was also in agreement with the calculated adsorption capacity ( $Q_{\rm cal}$ ) shown in Table 8. The slight difference between  $Q_{\rm exp}$  and  $Q_{\rm cal}$  further supports that chemisorption was the dominant adsorption mechanism<sup>48</sup>.

No	Biosorbent	Surface Area (m2/g)	Functional Groups	Qe (mg/g)	Removal Efficiency (%)	Reference
1	Banana Peel AC	21.456	OH, -COOH	0.323	89.41	15
2	waste orange	512.2	-СН, -ОН, -С-О, -СОО	33	98.4	49
3	Activated kenaf core fiber	-	-OH, C-H, C=C, C-O, C-O-C	303.03	99.8	50
4	Activated Bone char	-	-OH, -CH, -CO <sub>3</sub> , PO <sub>4</sub> <sup>3-</sup> , -NH	20.89	91.43	19
5	AC water hyacinth	-	-OH, C-H, -C=O, C-O-C, P = OOH	11.79	92.26	10
6	AC of CES	496.316	C=O,-OH, C=C, -PO <sub>4</sub>	7.94	94.5	Current study

**Table 9.** Comparison of the physiochemical properties AC of CES with various biosorbents.

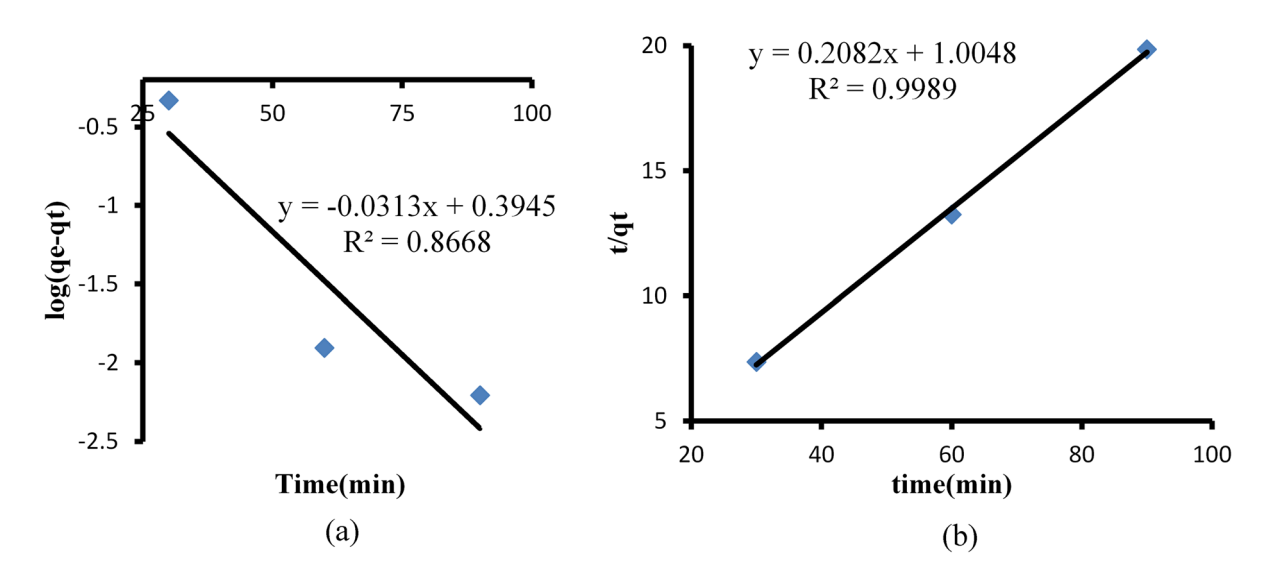


Fig. 8. Pseudo first order (a) and pseudo second order (b) adsorption plots of RR-45-D onto AC of CES.

Adsorbent	$\Delta H(K\theta.\mu o \lambda^{-1})$	ΔS (J.Mol <sup>-1</sup> .K <sup>-1</sup> )	ΔG [KJ.mol <sup>-1</sup> ]				
			298 K	303 K	318 K	333k	
AC	-166.06	-50.49	-1.367	0.314	2.24	4.79	

Table 10. Thermodynamic study of adsorption of RR-45-D onto the AC of CES.

The physicochemical properties of activated carbon CES including Surface Area, surface functional groups, adsorption capacity and percent of removal efficiency were compared with other biosorbents (Table 9).

### Thermodynamics study

The thermodynamic properties for the adsorption of RR-45-D onto the AC of CES were investigated in the temperature range of 298–333 K under optimum conditions(initial dye concentration 50.4 mg/L, pH 3.05, adsorbent dose 1.05 g and contact time 38.79 min). The adsorption capacity was decreased from 4.55 to 3.12 mg/g) as the temperature increased from 298 to 333 K as shown in Fig. 9a. A regression of Van't Hoff for thermodynamic parameters of RR-45-D adsorption onto the AC biosorbent is shown on Fig. 9b.

Table 10 shows the thermodynamic studies of adsorption of RR-45-D onto AC at the optimum conditions with varied temperature. The negative value of  $\Delta H$  (-166.06) confirmed that the adsorption process was exothermic and chemisorption type<sup>51</sup>. Because the adsorption energy was found in the range of -80 to 400 KJ/mol<sup>48</sup>. The exothermic nature of the reaction indicated that adsorption was more favorable at lower temperatures and less efficient at higher temperatures. This is consistent with the experimental data showing a decrease in adsorption efficiency with increasing temperature. The negative values of entropy ( $\Delta S = -50.49$ ) indicated a decrease randomness at the solid-solution interface during the adsorption of RR-45-D onto prepared AC adsorbent<sup>52</sup>. The  $\Delta G$  value for the removal of RR-45-Dwas negative at lower temperatures (298 K). This verifies that the adsorption of RR-45-D onto AC biosorbent was spontaneous and thermodynamically feasible at low temperatures. However, with increasing in temperature, the values of  $\Delta G$  were positive, which suggested that the equilibrium capacity was decreased due to desorption of adsorbed dyes<sup>53</sup>. This study was in agreement with the results observed for the adsorption of malachite green dye onto a novel low-cost gibto seed peel<sup>7</sup>. Additionally, it

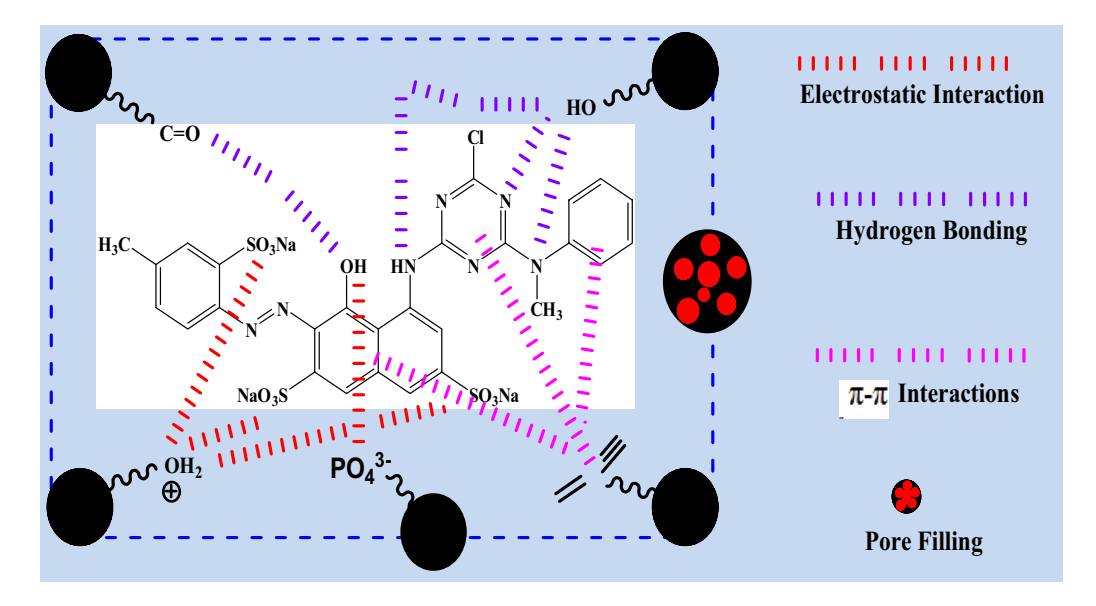
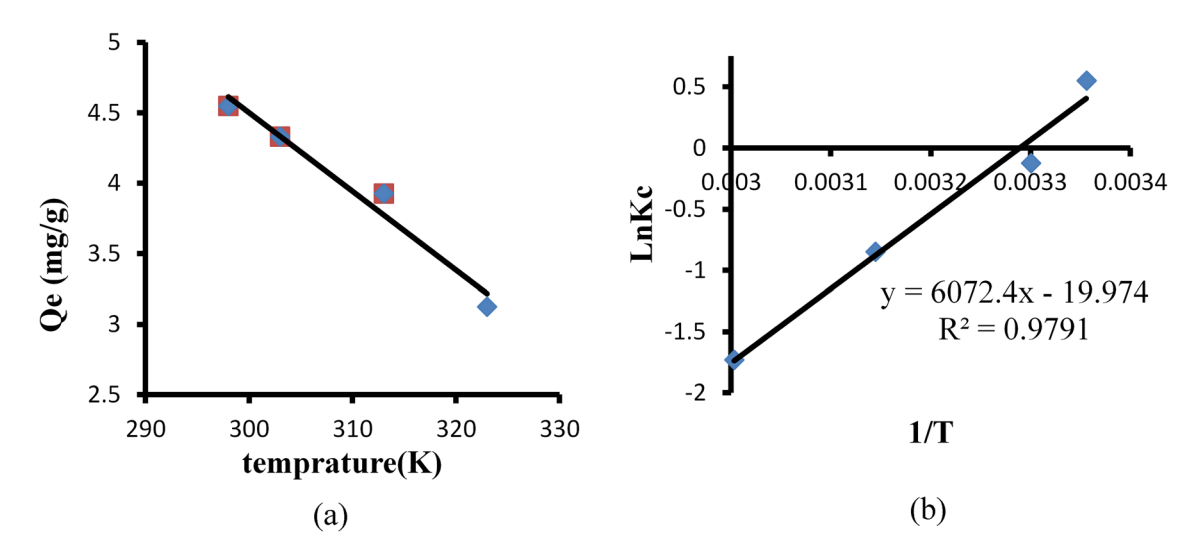


Fig. 10. Possible interaction mechanism between RR-45-D and AC from CES.



**Fig. 9.** Effect of temperature on adsorption capacity of AC of CES (a); Regressions of Van't Hoff for thermodynamic parameters of RR-45-D adsorption onto AC biosorbent (b).

also agrees with the results observed for the adsorption of reactive red dye from textile wastewater onto banana and orange peels $^{15}$ .

### Adsorption mechanism

The RR-45-D dye used in this study contains functional groups such as C=C bonds within aromatic rings, hydroxyl (-OH), sulfonate (-SO<sub>3</sub>), and amine (-NH) groups. The activated carbon (AC) derived from CES features functional groups including hydroxyl (-OH), aromatic C=C, and C=O, as identified through FTIR analysis. The presence of these varied functional groups enables multiple interaction mechanisms, including hydrogen bonding,  $\pi-\pi$  interaction (physisorption), and strong ionic or electrostatic interactions (chemisorption)<sup>48</sup> (Fig. 10).  $\pi-\pi$  interactions may arise between the aromatic C=C bonds in both the biosorbent and the RR-45-D dye. Electrostatic attraction may also occur between the positively charged sites on the AC of CES and the sulfonate (-SO<sub>3</sub>) groups of the dye, especially under acidic conditions (pH lower than the point of zero charge, pHzc < 4.82). Furthermore, hydrogen bonding is likely to occur between the highly electronegative oxygen and nitrogen atoms in the dye and functional groups on the biosorbent surface. Additionally, the adsorption process may include multiple diffusion mechanisms, such as bulk diffusion, boundary layer diffusion, thin-film diffusion, and intraparticle diffusion, which work together to transport RR-45-D molecules from the surrounding solution into the inner pores of the AC of CES.

### **Cost Estimation**

In this study, the CES, which is discarded as waste by khat leaf consumers, is collected at no cost. Activating 1 kg of this material requires around 300 mL of phosphoric acid, costing approximately 5 USD, along with 3 USD for carbonization and labor, bringing the total to 8 USD. In contrast, commercially available activated carbon, the most widely used adsorbent for adsorption purposes, is priced around 12 USD per kilogram<sup>54</sup>. Therefore, using the developed AC biosorbent is more cost-effective and offers a sustainable solution to environmental pollution issues.

### Conclusion

This study has investigated the removal efficiency of reactive red 45 dye on activated CES from aqueous solution. The biosorbent was prepared using phosphoric acid obeyed a surface area of 496.316 m<sup>2</sup>/g, which is good for reactive red dye removal in the wastewater. The physicochemical composition of the adsorbent including surface charge (point of zero charge), and available surface functional groups were investigated. The removal efficiency (%) of reactive red dye at different process parameters with their interaction effect was investigated and optimized using design expert software. The experimental data showed high removal efficiency (94.5%) at pH 3.05, adsorbent dose 1.05 gram, contact time 38.79 min, and initial dye concentration 50.4 mg/L. The adsorption equilibrium data were studied by adsorption isotherm, adsorption kinetics and adsorption thermodymics in order to know adsorbent capacity, adsorption rate and feasibility. Based on experimental result the adsorption process fits languimer isotherm model with pseudo- second-order kinetics model and it is thermodynamically feasible at low temperature. The ANOVA analysis revealed that bio-adsorption was highly affected by the solution pH, adsorbent dose, initial dye concentration, contact time and the interaction between the solution pH with other factors. In general, the AC prepared from CES showed strong potential for scale-up at the pilot level using actual textile wastewater containing Reactive Red 45 dye. However, additional studies such as Zeta potential analysis, column and regeneration experiments are necessary before considering full-scale implementation for textile wastewater treatment.

### Data availability

Data is provided within the manuscript.

Received: 23 January 2025; Accepted: 1 July 2025

Published online: 02 August 2025

### References

- Abate, G. Y., Alene, A. N., Habte, A. T. & Getahun, D. M. Adsorptive removal of malachite green dye from aqueous solution onto activated carbon of *Catha edulis* stem as a low cost bio-adsorbent. *Environ. Syst. Res.* 9 https://doi.org/10.1186/s40068-020-00191-4 (2020).
- 2. Nhung, N. T. H., Quynh, B. T. P., Thao, P. T. T., Bich, H. N. & Giang, B. L. Pretreated fruit peels as adsorbents for removal of dyes from water. IOP Conf. Ser. Earth Environ. Sci. 159 https://doi.org/10.1088/1755-1315/159/1/012015 (2018).
- Saravanan, A. et al. Adsorption characteristics of magnetic nanoparticles coated mixed fungal biomass for toxic Cr(VI) ions in aquatic environment. Chemosphere 267, 129226. https://doi.org/10.1016/j.chemosphere.2020.129226 (2021).
- 4. Fito, J., Said, H., Feleke, S. & Worku, A. Fluoride removal from aqueous solution onto activated carbon of Catha edulis through the adsorption treatment technology. *Environ. Syst. Res.* 8 https://doi.org/10.1186/s40068-019-0153-1 (2019).
- 5. Ramamurthy, K., Priya, P. S., Murugan, R. & Arockiaraj, J. Hues of risk: investigating genotoxicity and environmental impacts of Azo textile dyes. *Environ. Sci. Pollut Res.* 31 (23), 33190–33211 (2024).
- 6. 6Jawad, A. H., Razuan, R., Appaturi, J. N. & Wilson, L. D. Adsorption and mechanism study for methylene blue dye removal with carbonized watermelon (Citrullus lanatus)rind prepared via one-step liquid phase H<sub>2</sub>SO<sub>4</sub> activation. Surf Interfac 16,76–84 (2019); https://doi.org/10.1016/j.surfin.2019.04.012
- 7. Alene, A. N., Abate, G. Y. & Habte, A. T. Bioadsorption of basic blue dye from aqueous solution onto Raw and modified waste Ash as economical alternative bioadsorbent. *J. Chem. 1.* 8746035 https://doi.org/10.1155/2020/8746035 (2020).
- 8. 8Aragaw, T. A. & Bogale, F. M. Biomass-Based adsorbents for removal of dyes from wastewater: A review. Front. Environ. Sci. 9(); doi: https://doi.org/10.3389/fenvs.2021.764958. (2021).
- Chawla, H., Singh, S. K. & Haritash, A. K. Reversing the damage: ecological restoration of polluted water bodies affected by pollutants due to anthropogenic activities. *Environ. Sci. Pollut Res.* 31, 127–143. https://doi.org/10.1007/s11356-023-31295-w (2024).
- 10. Alemu, A. & Kerie, E. Removal of acid yellow 17 dye from aqueous solutions using activated water hyacinth (Eichhornia crassipes). Water Pract. Technol. 17 https://doi.org/10.2166/wpt.2022.063 (2022).
- 11. Dutta, S., Gupta, B., Srivastava, S. K. & Gupta, A. K. Recent advances on the removal of dyes from wastewater using various adsorbents: A critical review. *Materials Advances*, 4497–4531 (2021); https://doi.org/10.1039/d1ma00354b
- 12. Saini, R. D. Textile organic dyes: polluting effects and elimination methods from textile waste water. *Int J. Chem. Eng. Res* **9**(1), 121–136 (2017). http://www.ripublication.com
- 13. Alzain, H., Kalimugogo, V., Hussein, K. & Karkadan, M. A review of environmental impact of Azo dyes. *Int. J. Res. Rev.* 10 (6), 673–689. https://doi.org/10.52403/ijrr.20230682c (2023).
- Alhujaily, A., Yu, H., Zhang, X. & Ma, F. Adsorptive removal of anionic dyes from aqueous solutions using spent mushroom waste. *Appl. Water Sci.* 10 https://doi.org/10.1007/s13201-020-01268-2 (2020).
- 15. Temesgen, F., Gabbiye, N. & Sahu, O. Biosorption of reactive red dye (RRD) on activated surface of banana and orange peels: economical alternative for textile effluent. *Surf. Interfac.* 12, 151–159. https://doi.org/10.1016/j.surfin.2018.04.007 (2018).
- Zarghmapour, S., Khodadadi, A., Rahimpoor, R., Mengelizadeh, N. & Balarak, D. Photocatalytic activation of peroxymonosulfate by MOF-5@ Fe3O4 in the removal of acid blue 113 from polluted water. Results Eng. 25, 104426. https://doi.org/10.1016/j.rineng. 2025.104426 (2025).
- 17. Elahian, M., Ahmadi, N., Heidari, A. A., Mengelizadeh, N. & Balarak, D. Preparation of a polyaniline-supported Ce-Ag-doped ZnO nanocomposite for efficient photocatalytic degradation of acid blue 113 dye. *Results Eng.* 25, 103824. https://doi.org/10.1016/j.rineng.2024.103824 (2025).
- 18. Balarak, D., Ganji, F., Choi, S. S., Lee, S. M. & Shim, M. J. Effects of operational parameters on the removal of acid blue 25 dye from aqueous solutions by electrocoagulation. *Appl. Chem. Eng.* **30** (6), 742–748. https://doi.org/10.14478/ace.2019.1092 (2019).

- 19. Kerie, E. & Alemu, A. Removal of acid yellow dye 17 from aqueous solutions using an activated bone Char. Water Qual. Res. J. 57 https://doi.org/10.2166/wqrj.2022.016 (2022).
- 20. Karić, N. et al. Bio-waste valorisation: agricultural wastes as biosorbents for removal of (in) organic pollutants in wastewater
- treatment. Adv. Chem. Eng. 9, 100239. https://doi.org/10.1016/j.ceja.2021.100239 (2022).

  21. Velkova, Z., Lazarova, K., Kirova, G. & Gochev, V. Recent advances in pharmaceuticals biosorption on microbial and Algal-Derived biosorbents. Processes 13 (2), 561. https://doi.org/10.3390/pr13020561 (2025).
- Nawaz, S., Tabassum, A., Muslim, S., Nasreen, T., Baradoke, A., Kim, T. H., ... Bilal, M. Effective assessment of biopolymer-based multifunctional sorbents for the remediation of environmentally hazardous contaminants from aqueous solutions. Chemosphere, 329, 138552 (2023), https://doi.org/10.1016/j.chemosphere.2023.138552.
- 23. Akhtar, M. S., Ali, S. & Zaman, W. Innovative adsorbents for pollutant removal: exploring the latest research and applications. Molecules 29 (18), 4317. https://doi.org/10.3390/molecules29184317 (2024).
- 24. Mary Ealias, A., Meda, G. & Tanzil, K. Recent progress in sustainable treatment technologies for the removal of emerging contaminants from wastewater: A review on occurrence, global status and impact on biota. Rev Environ. Contam. Toxicol 262(1), 16 (2024), https://doi.org/10.1007/s44169-024-00067-z
- 25. Aziz, K. H. H. et al. Heavy metal pollution in the aquatic environment: efficient and low-cost removal approaches to eliminate their toxicity: a review. RSC Adv. 13 (26), 17595-17610. https://doi.org/10.1039/D3RA00723E (2023).
- 26. Yelatontsey, D. Production of versatile biosorbent via eco-friendly utilization of non-wood biomass. Chem. Eng. J. 451 https://doi. org/10.1016/j.cej.2022.138811 (2023).
- 27. Alemu, A., Lemma, B., Gabbiye, N., Alula, M. T. & Desta, M. T. Removal of chromium (VI) from aqueous solution using vesicular basalt: a potential low cost wastewater treatment system. Heliyon 4 (2018). https://doi.org/10.1016/j.heliyon.2018.e0068
- 28. Nigatu, Å. & Libsu, S. Studies on the effects of extracts of fresh khat/catha edulis leaves on the oxidation of niger seed oil. Pharm. Pharmacol., 7, 421-428(2019); (2019). https://doi.org/10.17265/2328-2150/2019.07.007
- 29. Alhogbi, B. G., Altayeb, S., Bahaidarah, E. A. & Zawrah, M. F. Removal of anionic and cationic dyes from wastewater using activated carbon from palm tree fiber waste. Processes 9 (3), 1-21. https://doi.org/10.3390/pr9030416 (2021).
- Dimbo, D. et al. Methylene blue adsorption from aqueous solution using activated carbon of spathodea campanulata. Results Eng. 21, 101910. https://doi.org/10.1016/j.rineng.2024.101910 (2024).
- 31. Hussain, Z. et al. Modification of coal fly Ash and its use as low-cost adsorbent for the removal of directive, acid and reactive dyes. J. Hazard. Mat. 422 ()126778; https://doi.org/10.1016/j.jhazmat.2021.126778 (2022).
- 32. Johnson, R. D. & Arnold, F. H. The Temkin isotherm describes heterogeneous protein adsorption. Biochimica. Et. Biophys. Acta (BBA)/ prot. Struct. Mol. 1247 (2), 293-297. https://doi.org/10.1016/0167-4838(95)00006-G (1995).
- 33. Lagergren, S. K. 1898 about the theory of so-called adsorption of soluble substances sven. Vetenskapsakad Handingarl. 24, 1-39 (1898)
- 34. Ho, Y. S. & McKay, G. Pseudo-second order model for sorption processes. Process Biochem. 34 (5), 451-465 (1999).
- 35. Alene, A. N., Abate, G. Y., Habte, A. T. & Getahun, D. M. Utilization of a novel low-cost Gibto (Lupinus Albus) seed Peel waste for the removal of malachite green dye: equilibrium, kinetic, and thermodynamic studies. J. Chem. 1, 6618510. https://doi.org/10.115 5/2021/6618510 (2021).
- 36. Kra, D. O., Atheba, P., Drogui, P. & Trokourey, A. Preparation and characterization of activated carbon based on wood (Acacia auriculeaformis, Côte d'Ivoire). J. Encapsul Adsorp Sci. 9 https://doi.org/10.4236/jeas.2019.92004 (2019)
- 37. Alemu, A., Lemma, B. & Gabbiye, N. Adsorption of chromium (III) from aqueous solution using vesicular basalt rock. Cogent Environm Scie 5 (), 1650416. https://doi.org/10.1080/23311843.2019.1650416 (2019).
- 38. Balarak, D., Zafariyan, M., Igwegbe, C. A., Onyechi, K. K. & Ighalo, J. O. Adsorption of acid blue 92 dye from aqueous solutions by single-walled carbon nanotubes: isothermal, kinetic, and thermodynamic studies. Environ. Process. 8, 869-888. https://doi.org/10 .1007/s40710-021-00505-3 (2021).
- 39. Yetgin, S. & Amlani, M. Agricultural low-cost waste adsorption of methylene blue and modelling linear isotherm method versus nonlinear prediction. Clean. Technol. Environ. Policy. 1-21. https://doi.org/10.1007/s10098-024-02928-6 (2024).
- 40. Ecer, Ü., Yılmaz, Ş. & Şahan, T. Synthesis, characterization, and application of Ag-doped mercapto-functionalized clay for decolorization of coomassie brilliant blue: optimization using RSM. Chem Phys. Lett. 825, 140610. https://doi.org/10.1016/j.cplett
- 41. Kumari, S. & Annamareddy, S. H. K. Treatment of garage wastewater using activated carbon made from Khat (Catha edulis) and Neem (Azadirachta indica) leaves. Environ. Dev. Sustain. 22 https://doi.org/10.1007/s10668-019-00330-7 (2020).
- Shamsuddin, M. S., Yusoff, N. R. N. & Sulaiman, M. A. Synthesis and characterization of activated carbon produced from Kenaf core Fiber using H3PO4 activation. Procedia Chem. 19, 558-565. https://doi.org/10.1016/j.proche.2016.03.053 (2016).
- Bykov, M. et al. Crystal structures of cristobalite-type and coesite-type PON redetermined on the basis of single-crystal X-ray diffraction data. Acta Crystallogr. E: Crystallogr. Commun., 71(); https://doi.org/10.1107/s205698901501899x (2015).
- Yihunu, E. W., Minale, M., Abebe, S. & Limin, M. Preparation, characterization and cost analysis of activated Biochar and hydrochar derived from agricultural waste: a comparative study. SN Appl. Sci. 1,1-8 (), https://doi.org/10.1007/s42452-019-0936-z
- Abdulsalam, K. A., Giwa, A. R. A. & Adelowo, J. M. Optimization studies for decolourization of textile wastewater using a sawdustbased adsorbent. Chem. Data Collect. 27() 100400, https://doi.org/10.1016/j.cdc.2020.100400 (2020).
- 46. Behnamfard, A., Chegni, K., Alaei, R. & Veglio, F. The effect of thermal and acid treatment of Kaolin on its ability for cyanide removal from aqueous solutions. Environ. Earth Sci. 1-12 https://doi.org/10.1007/s12665-019-8408-8 (2019).
- 47. Fito, J. et al. Adsorption of methylene blue from textile industrial wastewater using activated carbon developed from Rumex
- abyssinicus plant. *Sci. Rep.* **13** (1), 5427. https://doi.org/10.1038/s41598-023-32341-w (2023). Sudarsan, S., Murugesan, G., Varadavenkatesan, T., Vinayagam, R. & Selvaraj, R. Efficient adsorptive removal of congo red dye using activated carbon derived from Spathodea campanulata flowers. Sci. Rep. 15 (1), 1831 (2025).
- Ramutshatsha-makhwedzha, D., Mavhungu, A., Moropeng, M. L. & Mbaya, R. Activated carbon derived from waste orange and lemon peels for the adsorption of Methyl Orangeand Methylene blue dyes from wastewater. Heliyon, 8(8)(2022), e09930. https://d oi.org/10.1016/j.heliyon.2022.e09930
- 50. Idan, I. J., Abdullah, L. C., Choong, T. S. & Jamil, S. N. A. B. M. Equilibrium, kinetics and thermodynamic adsorption studies of acid dyes on adsorbent developed from Kenaf core fiber. Adsorp Sci. Technol. 36 (1-2), 694-712. https://doi.org/10.1177/0263617 417715532 (2017)
- 51. Lian, L. L., Guo, L. P. & Guo, C. J. Adsorption of congo red from aqueous solutions onto Ca-bentonite. J. Hazard. Mater. 161 https://doi.org/10.1016/j.chm.2016.1016. ://doi.org/10.1016/j.jhazmat.2008.03.063 (2009).
- 52. Balarak, D., Zafariyan, M., Igwegbe, C. A., Onyechi, K. K. & Ighalo, J. O. Adsorption of acid blue 92 dye from aqueous solutions by single-walled carbon nanotubes: isothermal, kinetic, and thermodynamic studies. Environ. Processes. 8, 869-888. https://doi.org/1 0.1007/s40710-021-00505-3 (2021)
- 53. Ecer, Ü. & Yılmaz, Ş. Fabrication of magnetic biochar-MIL-68 (Fe)-supported Cobalt composite material toward the catalytic reduction performance of crystal Violet. J. Water Process. Eng. 57, 104574. https://doi.org/10.1016/j.jwpe.2023.104574 (2024).
- Sahu, N. et al. Adsorption of as (III) and as (V) from aqueous solution by magnetic biosorbents derived from chemical carbonization of pea Peel waste biomass: isotherm, kinetic, thermodynamic and breakthrough curve modeling studies. J. Environ. Manag. 312, 114948. https://doi.org/10.1016/j.jenvman.2022.114948 (2022).

### **Acknowledgements**

The authors are grateful to Bahir Dar University for financing lab analysis.

### **Author contributions**

AA &TM developed the concept, AA, TM, NG, BT, and DT, prepared the draft and revised the manuscript. All authors have contributed to this paper and approved submission.

### **Declarations**

### Competing interests

The authors declare no competing interests.

### Additional information

Correspondence and requests for materials should be addressed to A.A.

Reprints and permissions information is available at www.nature.com/reprints.

**Publisher's note** Springer Nature remains neutral with regard to jurisdictional claims in published maps and institutional affiliations.

Open Access This article is licensed under a Creative Commons Attribution-NonCommercial-NoDerivatives 4.0 International License, which permits any non-commercial use, sharing, distribution and reproduction in any medium or format, as long as you give appropriate credit to the original author(s) and the source, provide a link to the Creative Commons licence, and indicate if you modified the licensed material. You do not have permission under this licence to share adapted material derived from this article or parts of it. The images or other third party material in this article are included in the article's Creative Commons licence, unless indicated otherwise in a credit line to the material. If material is not included in the article's Creative Commons licence and your intended use is not permitted by statutory regulation or exceeds the permitted use, you will need to obtain permission directly from the copyright holder. To view a copy of this licence, visit <a href="http://creativecommons.org/licenses/by-nc-nd/4.0/">http://creativecommons.org/licenses/by-nc-nd/4.0/</a>.

© The Author(s) 2025